4.1.1.6 Quiet and slowly varying radio emissions of the sun

Arnold O. Benz

The solar atmosphere emits radio emission at all wavelengths and at all times. Its total flux density varies with magnetic activity as manifest in sunspots. At every wavelength there is a well-defined minimum radiation level. It is reached when the sun has been free of spots for some weeks. This is called the *quiet* radio emission of the sun. The presence of sunspots enhances the radio emission, producing a *slowly variable* component.

Both quiet and slowly varying radio emissions are thermal radiations. As all radio emission becomes optically thick at some level in the atmosphere, the brightness temperature (proportional to the radiation intensity in the Rayleigh-Jeans approximation) corresponds to a mean temperature weighted over a density range given by the wavelength. Contrary to non-thermal emission, the brightness temperature of thermal emission cannot exceed the plasma temperature. Thermal emission originates at an altitude that depends on wavelength: the longer the wavelength, the higher the dominant altitude of emission. As the temperature increases with altitude from the chromosphere into the corona, so does the radio brightness temperature with longer wavelengths. At centimeter wavelengths and smaller, the radiation originates from the chromosphere, having chromospheric brightness temperature. At meter waves and longer, the radiation originates in the corona.

Thermal radiation is occasionally outshone for a time of some milliseconds to hours by much brighter emission of a population of high-energy electrons having a *non-thermal* energy distribution produced by coronal activity: the disturbed components of the solar radio emission are described in Section 3.1.2.8. It may be noted here that the electron energy distribution in the quiet corona is predicted to have super-thermal tails, causing the emission to deviate from a purely thermal radiation [04Chi]. Finally, nanoflares in quiet regions add non-thermal emission at centimeter wavelengths, that is however more than a million times smaller than the full-disk thermal emission [00Kru].

4.1.1.6.1 Flux density of the quiet sun full disk radio emission

The quiet emission establishes a minimum radiation level produced by thermal bremsstrahlung (free-free emission) in the atmosphere. Solar poles are always devoid of spots, thus are quiet. In the equatorial zone up to 50° latitude, sunspots appear and disappear at solar activity minimum. The flux level of the total quiet sun thus refers to the total emission of the sun at sunspot minimum. Corrected for the variable sun-earth distance, it is the component of the solar radio emission that is constant in time. As the quiet solar emission is the strongest source in the sky at meter wavelengths and below, it is often used to calibrate small single dish telescopes.

The values in Table 1 for the quiet radio flux density, $F_\odot$, are based on measurements made during the sunspot years 1964 and 1976. The data were collected from various telescopes around the globe [81Hac1]. The quiet solar radio emission is not an active research field today, but the measurements from decades ago are still trustworthy. The flux measurements of Table 1 at wavelengths $\lambda > 1$ cm are based on measurements from [69Leb, 75Lan, 77Kun1, 77Eri, 65Kru, 73Tan]. The absolute values of the radiation flux in this range of wavelengths are usually calibrated with intense galactic and extragalactic radio sources. The residuals about the mean curve, mostly due to calibration errors, amount to about ±7%. At millimeter wavelengths, the moon is usually used for calibration. Millimeter measurements [71Reb, 73Lin, 76Kus] are presented in Table 1. The data were smoothed in wavelength. The deviations of the measurements about this mean curve was about ±5%. Thus the total accuracy of Table 1 is about 10%. More recent observations [91Zir, 92Bor] report values within the estimated errors.

Table 1. Flux density, $F_\odot$, and brightness temperature, T_{rad}, of the quiet sun.
$F_\odot$ = radio flux density of the quiet sun during sunspot minimum in units of 10^{-22} W m^{-2} Hz^{-1} = 10^{-19} erg cm^{-2} Hz^{-1} s^{-1} = solar flux unit (sfu)
T_{rad} = brightness temperature of an optical solar disk with a diameter of $32'$
T_c = brightness temperature at the center of the solar disk
T_h = brightness temperature in a coronal hole
Where necessary, the values have been interpolated assuming a λ^2 wavelength dependence (Rayleigh-Jeans approximation).

f [MHz]	λ [cm]	$F_\odot$ [sfu]	T_{rad} [K]	T_c [K]	T_h [K]
30	1000	0.17	$9.03 \cdot 10^5$	$5.1 \cdot 10^5$	$5.1 \cdot 10^5$
50	600	0.54	$10.3 \cdot 10^5$	$6.2 \cdot 10^5$	$6.2 \cdot 10^5$
100	300	2.4	$11.5 \cdot 10^5$	$8.9 \cdot 10^5$	$6.7 \cdot 10^5$
150	200	5.1	$11.0 \cdot 10^5$	$9.5 \cdot 10^5$	$6.4 \cdot 10^5$
200	150	8.1	$9.7 \cdot 10^5$	$8.6 \cdot 10^5$	$6.1 \cdot 10^5$
300	100	14.9	$7.9 \cdot 10^5$	$7.0 \cdot 10^5$	$5.4 \cdot 10^5$
400	75	21.7	$6.5 \cdot 10^5$	$5.6 \cdot 10^5$	$4.4 \cdot 10^5$
600	50	32.1	427000	363000	265000
1000	30	41.3	197000	162000	108000
1500	20	48.0	102200	83800	57800
3000	10	69	36680	31180	25100
3750	8	82	27900	24550	20770
5000	6	107	20670	18810	16650
10000	3	275	13160	12240	11700
15000	2	574	12210	11600	11360
20000	1.5	890	11560	11100	
30000	1.0	1862	10480	10110	
37500	0.8	2816	9580	9290	
50000	0.6	4503	8619	8450	
100000	0.3	14709	7038	6900	
300000	0.1	113200	6018	5900	

The radio flux density, $F_\odot$, and the corresponding brightness temperature, T_{rad}, are related by

$$F_\odot = 2.09 \cdot 10^{-44} f^2 T_{rad} \quad , \tag{1}$$

where $F_\odot$ is in units of [W m^{-2} Hz^{-1}], the frequency f in [Hz], and T_{rad} in [K].

The temperature T_c at disk center was derived from $F_\odot$ using the known brightness distribution over the solar surface (see also 4.1.1.6.2). Some values for T_c in the millimeter and meter ranges were obtained from direct measurements and adjusted. At the lowest frequencies, scattering on irregularities in the corona increases the size of the solar disk and reduces the brightness temperature [71Aub, 08The].

According to definition, the brightness temperature T_c in the center of the solar disk refers to a surface without active regions but showing arc structures in the corona. In regions of coronal holes having open magnetic configurations, the brightness temperature is reduced to T_h. Reductions were inferred according to [76Fue, 77Dul, 78Tro].

The quiet solar radio flux density, $F_\odot$, is graphically displayed in Fig. 1. It has three distinct regions: (*i*) At frequencies higher than 6000 MHz, the emission originates mainly in the chromosphere, following the f^2 Rayleigh-Jeans approximation of a blackbody of 6000 to 10000 K. (*ii*) Below 350 MHz, the spectrum is approximately an f^2 power law and corresponds to the one million degree quiet corona. (*iii*) In between, there is a transition region from predominantly

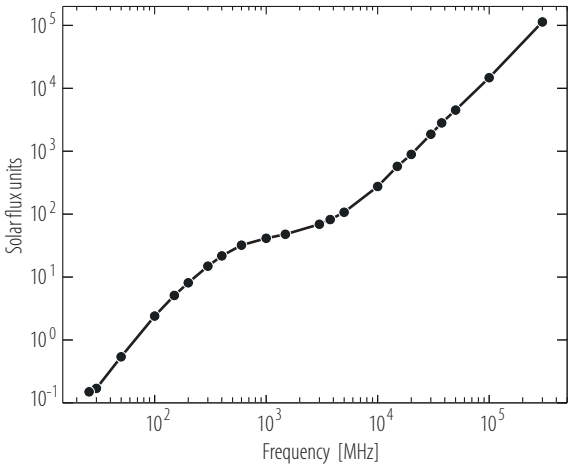

Fig. 1. Spectrum of quiet solar radio flux density, $F_\odot$, based on the values presented in Table 1. A solar flux unit (sfu) is 10^{-22} W m^{-2} Hz^{-1} $= 10^{-19}$ erg cm^{-2} Hz^{-1} s^{-1}.

chromospheric, to transition region radiation and finally to predominantly coronal emission. The quiet solar radio flux density can be approximated in the three regions by

$$F_\odot = 1.94 \cdot 10^{-4} f^{1.992}\ , \quad 30 - 350 \text{ MHz}, \tag{2}$$

$$F_\odot = 8.45 \cdot 10^{-1} f^{0.5617}\ , \quad 350 - 6000 \text{ MHz}, \tag{3}$$

$$F_\odot = 2.79 \cdot 10^{-5} f^{1.748}\ , \quad 6000 - 400000 \text{ MHz}, \tag{4}$$

where $F_\odot$ is in units of [sfu] ($= 10^{-22}$ W m^{-2} Hz^{-1}) and the frequency f is in [MHz]. The observed polarization of the total quiet sun radiation is zero, in accordance with theory.

4.1.1.6.2 Brightness distribution across the quiet solar disk

Radio maps of the sun include radiation of the quiet sun and enhanced emissions of active regions. The latter change in shape and intensity on a time scale of a day. Here we focus on the brightness distribution of the quiet sun across the disk visible from Earth. We proceed from the shortest radio wavelengths originating lowest in the solar atmosphere to the longest wavelengths emitted high in the corona.

a) Smoothed brightness distribution observed at millimeter waves

At millimeter waves, the brightness of the disk is on the average uniform for about $R < 0.8 R_\odot$. Beyond that radius, limb darkening is observed. It has been interpreted by the height of the emission increasing radially on the disk. As the temperature in the lower chromosphere decreases with altitude, the brightness decreases as well. Eclipse observations (Fig. 2) near the longer end of the millimeter range indicate a faint bright ring at the edge of the disk superimposed over the limb darkening [57Hag, 77Kun2, 72Lan]. It is possibly caused by chromospheric spicules, vertical jets seen in projection at the limb.

b) Smoothed brightness distribution observed at centimeter and decimeter waves

In centimeter wavelengths the radio image of the quiet sun becomes slightly elliptical. At $\lambda =$ 2.8 cm the radius measures 1.04 $R_\odot$ (photospheric radii) at the equator, and 1.01 $R_\odot$ at the meridian (N-S direction) (Fig. 3). The emission is radiated higher in the chromosphere than in millimeter waves and in a region, where temperature increases with height. Thus limb brightening is clearly visible. In decimeter waves, the emission of the spicules is negligible. There is still a peak

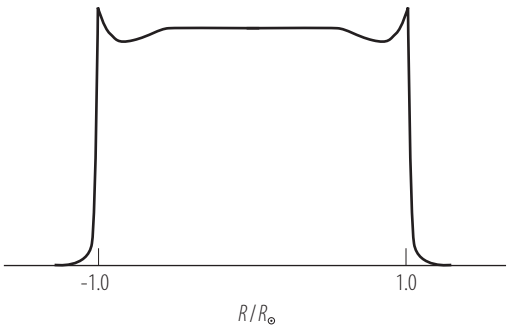

Fig. 2. Brightness distribution of quiet solar radio emission at $\lambda = 8.5$ mm. The profile is derived from an eclipse observation, assuming a circularly symmetric distribution [57Hag].

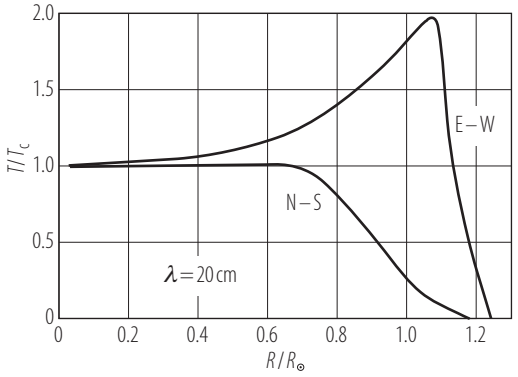

Fig. 3. Brightness distribution of quiet solar radio emission at a wavelength of 20 cm (1.5 GHz) at solar minimum. The profile is derived from single-dish scans in North-South and East-West with the 100 m telescope in Effelsberg [81Hac1].

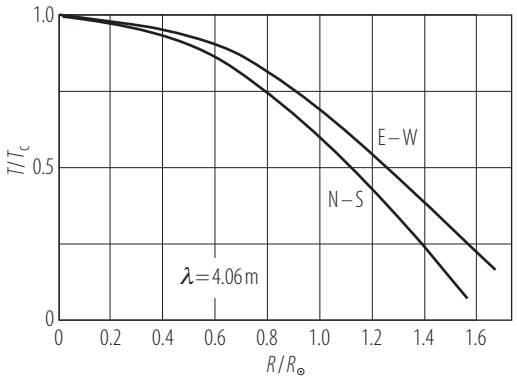

Fig. 4. Brightness distribution of quiet solar radio emission at 4.06 m wavelength (73.9 MHz). The profile is derived from interferometric observation by the Clark Lake Radio Observatory [77Kun1].

at low latitudes, but its maximum is at a radius beyond the limb and is caused by a contribution of the corona. Its contributed brightness increases with wavelength and is smaller in the polar regions where coronal holes and out-flowing solar wind reduce the density.

c) Smoothed brightness distribution observed at meter and decameter waves

Figure 4 displays two profiles at meter waves. All the emission originates in the corona and thus extends beyond $R_\odot$.

At meter wavelengths and longer, the refractive index is less than unity over a significant part of the ray path. Thus refraction and scattering bend the ray paths in outward direction. Non-central rays turn aside from a straight line, avoid the denser part of the corona and leave the corona, before the optical depth τ becomes unity. Thus the corona is not optically thick at 100 MHz and below. The corona then is not a blackbody anymore and the brightness temperature $T_{\rm rad}$ decreases to $T_{\rm rad} = T_e(1 - e^{-\tau})$ where T_e is the coronal electron temperature.

Scattering on small inhomogeneities, and to a lesser extend refraction, increase the apparent source size. The radio emission of the quiet sun becomes spread out [85She]. Scattering may be enhanced by anisotropy of the dense regions, extending in bundles along the magnetic field. The low density parts duct the radiation before escaping and reduce the brightness temperature by a factor of $1/f$, where f is the filling factor [88Mel], as the scattering prohibits rays to penetrate to where the optical depth is large. The effect of scattering progressively increases away from disk center. Therefore, the brightness temperature decreases from the center to the limb.

d) The radio radius of the sun

The solar radius in radio waves may be defined as the radius of the isophote $T_{\rm rad} = 0.5T_c$ at the limb. It is usually given in units of the photospheric radius $R_\odot$. The values in E-W start to deviate considerably from N-S at centimeter wavelengths and longer due to the coronal contribution (Fig. 5). In polar latitudes, where the coronal density is lower than at the equator, the decimeter radio radius is therefore smaller than 1 $R_\odot$ according to the above definition (see Fig. 3). The effect of solar oblateness is of the order of 10^{-5} [08Fiv] and is not relevant for the accuracy considered in Fig. 5. The data in Fig. 5 have been collected from various observations [81Hac1]. The observations include single-dish measurements at millimeter waves, eclipse observations at centimeter and decimeter waves and interferometric observations at meter waves.

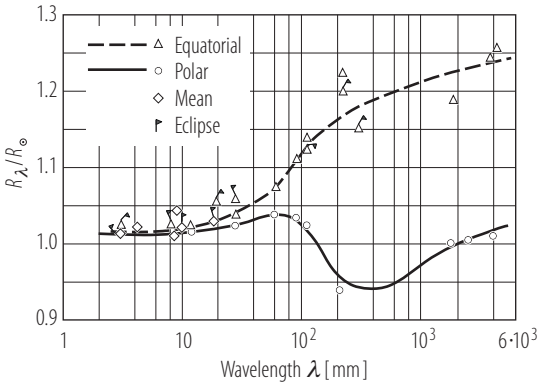

Fig. 5. The equatorial and polar radio radius of the quiet sun vs. wavelength [81Hac1].

Both the equatorial and the polar radius increase starting around 10 mm (Fig. 5), due to the coronal contribution. The polar size decreases beyond 100 mm as the spicules become unimportant and the altitude of emission moves up into a region with lower temperature. Note that the radius increases considerably with wavelengths longer than 10 cm at solar maximum even in the absence of an active region at the limb.

e) Localized structures in the quiet sun

We note finally that the radio brightness distribution is slightly modulated by structures even in regions completely devoid of activity [88Gar]. In the chromosphere, the emission of millimeter and centimeter waves is enhanced at supergranules boundaries where also the most energetic nanoflares occur [97Ben]. Coronal holes reduce the radio emission at wavelengths from millimeter to meter waves [74Dul], but may enhance the brightness at wavelengths longer than about 10 meters [87Lan]. In centimeter waves, prominences and other low temperature features in the corona absorb the radiation originating in the upper chromosphere and produce “Low Temperature Regions” with reduced brightness [76But, 86Kun, 99Bra]. At 8 mm wavelength, the brightness variations across the quiet disk amount to ± 2% [78Hac].

4.1.1.6.3 Slowly varying radio emission of the sun

The slowly varying component of solar radio emission (often abbreviated to ”S-component”) is the total radio emission minus the quiet emission and the rapidly varying flare emission. The S-component originates in active regions, usually associated with sunspots and/or chromospheric plages. The spectral range over which the S-component is significant as compared to the radio flux of the quiet sun is

400 MHz $< f <$ 20 GHz
75 cm $>$ λ $>$ 1.5 cm

4.1.1.6.3.1 Properties of slowly varying emission

- Typical size[1]: $10^5 - 2 \cdot 10^5$ km
- Typical angular size: $2'$ - $4'$
- Maximum height above photosphere[2]: 70000 km at $\lambda = 3$ cm, 140000 km at $\lambda = 20$ cm
- The emission region consists of one or more bright centers surrounded by a halo. The halo becomes more prominent at wavelengths beyond 3 cm. The emission centers are located above regions of maximum magnetic field strength in the photosphere, i.e. primarily above sunspots. They have a size of $10''$ to $40''$ (7000 km to 30000 km).
- The polarization of the S-component is partially circular and originates mostly from the centers. Its sense of polarization corresponds to the extraordinary mode of the magneto-ionic theory.

The enhancement of the flux density of the total solar radiation in the decimeter and centimeter ranges is given in Table 2. The S-component relative to the quiet sun radio emission is strongest at 2800 MHz (10.7 cm). This is also the frequency where the correlations of the radio emission with the sunspot number (Table 2) and the ionization index of the E-layer (Fig. 6) have broad peaks. The value of the 10.7 cm flux is reported daily by the Dominion Radio Observatory [08Pen].

An S-component can also be recognized as a relative brightening of active regions in maps at millimeter wavelength. The increase of the brightness temperature relative to the surrounds is

Table 2. Enhancement of the radio emission of the Sun by solar activity: slowly varying component. The enhancement factors relative to the quiet solar emission are given for a 10.7 cm flux density of 240 sfu, corresponding to a relative sunspot number $R = 199$.
$F_\odot$ = radio flux density of the full quiet sun during sunspot minimum
F_{max} = radio flux density at a high level of solar activity
The correlation with the relative sunspot number is also shown [81Hac2].

f [MHz]	λ [cm]	Enhancement $F_{max}/F_\odot$	Correlation coefficient
500	60	2.07	little
1000	30	2.99	0.981
1500	20	3.36	
2000	15	3.48	
2800	11		0.997
3000	10	3.26	
3750	8		0.990
5000	6	2.75	
9400	4		0.973
10000	3	1.37	
17000	1.7		0.490
20000	1.5	1.10	

[1] Derived from solar eclipse observations by [63Hac].
[2] The source area of the enhanced emission correlates well with the area of the associated plages [57Chr].

on the average 300 K at 1 mm, 600 K at 5 mm, and 900 K at 8 mm [70Kun, 71Kun1, 71Kun2]. For full sun measurements, however, these enhancements amount to an increase of less than one percent.

4.1.1.6.3.2 Interpretation of the emission

The S-component has a brightness temperature corresponding to the region of emission. It does not exhibit the rapid time variations typical of burst phenomena known as "disturbed solar radiation". Thus it is generally interpreted as a thermal emission. There are two thermal processes responsible for the S-component: gyromagnetic emission and collisional bremsstrahlung.

Gyromagnetic emission is caused by the spiraling motion of thermal electrons around the magnetic field. The emission is radiated at low harmonics s of the electron gyrofrequency, Ω_e

$$\omega = s\Omega_e = s\frac{eB}{m_e c} = 2\pi \cdot 2.80 \cdot 10^6 sB \quad [\mathrm{s}^{-1}], \tag{5}$$

where cgs units are used and B is in units of [Gauss].

The emissivity decreases with harmonic number. Most efficient is the harmonic where the radiation becomes optically thick. This depends on frequency and angle between emission and magnetic field. Gyromagnetic radiation is circularly polarized in the extraordinary mode if temperature increases in height. The bright emission centers are generally interpreted as sources of this emission.

Bremsstrahlung emission is radiated above the $\tau = 1$ level of gyromagnetic emission. It is caused by velocity changes due to Coulomb collisions of thermal electrons. Bremsstahlung contributes a varying fraction to the total emission, depending on how much material there is in front of the $\tau = 1$ level of gyromagnetic emission. Both modes are emitted, but the ordinary mode becomes optically thick at a higher altitude. If the temperature increases with altitude, bremsstrahlung radiation is weakly polarized in the ordinary mode. The halo of the S-component emission is generally interpreted by thermal bremsstrahlung radiation of the higher than average density in the active region corona, called "coronal condensation".

4.1.1.6.3.3 Correlation of the S-component with other emissions

The importance of the 10.7 cm flux measurements is demonstrated in Fig. 6. The ionization of the terrestrial E-layer is caused by solar X-ray and UV irradiation originating in the corona and transition region. Thus Fig. 6 shows the correlation of the ionization index J_E with the radio emission and suggests that the high-energy irradiation responsible for E-layer ionization is causally linked to the origin of the 30-cm solar radio emission (1 GHz), i.e. in the lowest part of the corona and the transition region.

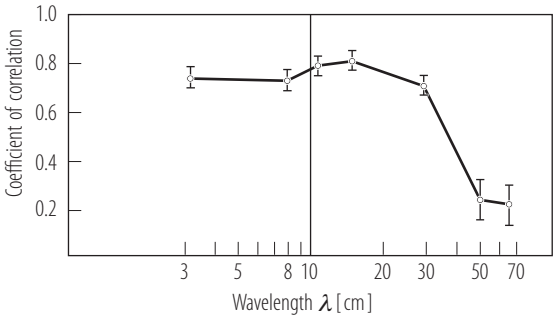

Fig. 6. Correlation coefficient between 5-day mean values of the ionization index of the terrestrial E-layer, J_E, and solar radio emission versus wavelength [60Kun].

Figure 7 shows another important relation, involving an even lower layer of the sun. The correlation of the radio emission with the total solar irradiation (including optical, UV and infrared) measured at Earth is highly significant (R=0.96). The daily radio flux at 10.7 cm is reported to be accurate to 1 % or 1 sfu, whichever is larger [01Tap]. As it is much easier to measure and dates back more than 60 years (Table 3), it can be used as a proxy for solar irradiation variability.

Table 2 indicates a good correlation of the full sun radio emission above 1 GHz with the monthly averaged sunspot number N_s. The correlation between the radio flux at 10.7 cm (2.8 GHz), $F_{10.7}$,

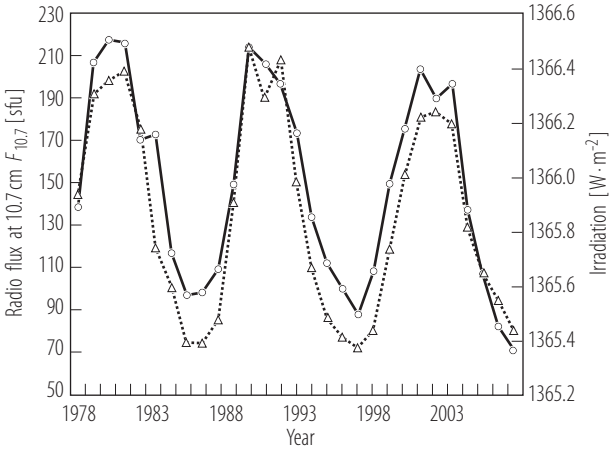

Fig. 7. Annually averaged solar radio emission at $\lambda = 10.7$ cm of S-component and quiet sun (*dashed line and open triangles*). Temporary bursts are excluded. Also shown is the total solar irradiation (*solid line and circles*) vs. time. The data has been scaled and shifted in y direction to show the correlation [07Tap].

Table 3. The solar radio flux density is measured daily at local noon in Penticton, BC, Canada. The measurements started on February 14, 1947, then still near Ottawa. The given values are yearly averages and exclude bursts. They are adjusted to a solar distance of one Astronomical Unit [08Tap].

Year	Flux density [sfu]	Year	Flux density [sfu]	Year	Flux density [sfu]
1947	220.56	1968	149.11	1989	213.42
1948	175.07	1969	151.14	1990	189.81
1949	177.61	1970	155.98	1991	208.03
1950	128.20	1971	118.22	1992	149.94
1951	119.71	1972	120.92	1993	109.56
1952	85.68	1973	93.35	1994	85.62
1953	73.85	1974	86.65	1995	77.15
1954	70.28	1975	76.13	1996	72.00
1955	95.64	1976	73.37	1997	80.73
1956	184.67	1977	86.94	1998	118.41
1957	232.81	1978	143.47	1999	153.96
1958	231.98	1979	191.58	2000	181.05
1959	210.32	1980	198.51	2001	183.64
1960	162.06	1981	202.59	2002	180.10
1961	105.51	1982	174.84	2003	130.09
1962	90.50	1983	119.89	2004	107.07
1963	81.30	1984	100.91	2005	94.60
1964	72.54	1985	74.75	2006	80.51
1965	76.36	1986	73.99	2007	73.05
1966	102.24	1987	85.35	2008	69.73
1967	143.24	1988	141.08		

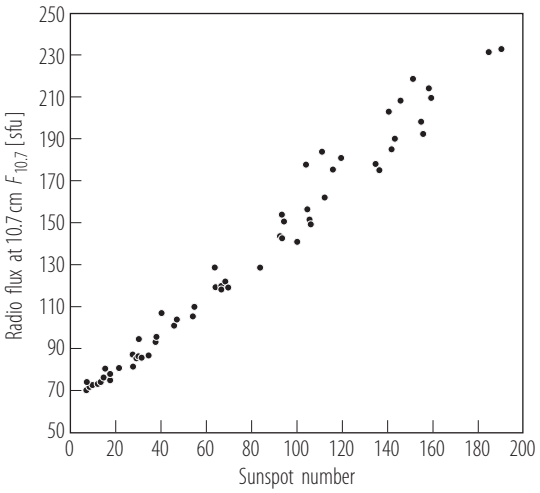

Fig. 8. Annually averaged solar radio emission at $\lambda = 10.7$ cm since 1947 (S-component and quiet sun, excluding temporary bursts) vs. sunspot number. A polynomial fit is also shown [01Tap].

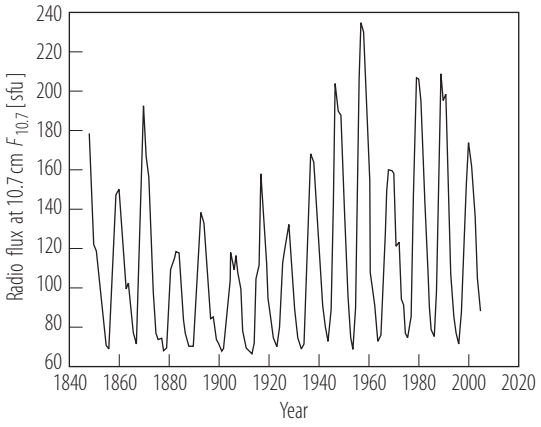

Fig. 9. S-component solar radio emission at $\lambda = 10.7$ cm (including quiet sun, in sfu) inferred from sunspot numbers, using the conversion Eq. (6) [08Zha].

and N_s is presented graphically in Fig. 8. It can be mathematically expressed by the equation

$$F_{10.7} = 67.0 + 0.572\ N_s + (0.0575\ N_s)^2 - (0.0209\ N_s)^3 \quad \text{[sfu]}. \tag{6}$$

The reverse equation is

$$N_s = 1.61\ F_{10.7} - (0.0733\ F_{10.7})^2 + (0.0240\ F_{10.7})^3 \quad . \tag{7}$$

The excellent correlation between sunspot number and radio flux allows using the sunspot number as a proxy for historical values of the 10.7 cm radio flux. This has been done in Fig. 9.

4.1.1.6.4 References for 4.1.1.6

General references

a Kundu, M.R.: *Solar Radio Astronomy* (1971), New York: Interscience Publishers, Chap. 6.

b Sheridan, K.V., McLean, D.J.: in *Solar Radiophysics* (McLean, D.J., Labrum, N.R., eds.), Cambridge: Cambridge University Press (1985) Chap. 17.

Special references

57Chr Christiansen, W.N., Warburton, J.A., Davies, R.D.: Austral. J. Phys. **10** (1957) 491.

57Hag Hagen, J.P.: in: *Radio Astronomy* IAU Symposium No. 4 (1957) (ed. H.C. Van de Hulst), Cambridge University Press, p. 263.

60Kun Kundu, M.R.: J. Geophys. Res. **65** (1960) 3903.

63Hac Hachenberg, O., Popowa, M., Prinzler, H.: Z. Astrophys. **58** (1963) 36.

65Kru Krüger, A., Michel, H.-St.: Nature **206** (1965) 601.

69Leb Leblanc, Y., Le Squeren, A.M.: Astron. Astrophys. **1** (1969), 239.

70Kun Kundu, M.R.: Solar Phys. **13** (1970) 348.
71Aub Aubier, M., Leblanc, Y., Boischot, A.: Astron. Astrophys. **12** (1971) 435.
71Kun1 Kundu, M.R.: Solar Phys. **21** (1971) 130.
71Kun2 Kundu, M.R.: in: *Solar Magnetic Fields* (Howard R., ed.) IAU Symp. No. **43** (1971), Reidel, Dordrecht, 642.
71Reb Reber, E.E.: Solar Phys. **16** (1971) 75.
72Lan Lantos, P., Kundu, M.R.: Astron. Astrophys. **21** (1972) 119.
73Lin Linsky, J.L.: Solar Phys. **28** (1973) 409.
73Tan Tanaka, H., Castelli, J.P., Covington, A.E., Krüger, A., Landecker, T.L., Tlamicha, A.: Solar Phys. **29** (1973) 243.
74Dul Dulk, G.A., Sheridan, K.V.: Solar Phys. **36** (1974) 191.
75Lan Lantos, P., Avignon, Y.: Astron. Astrophys. **41** (1975) 137.
76But Butz, M., Hirth, W., Fürst, E.: Mitt. Astr. Ges. **38** (1976) 211.
76Fue Fürst, E., Hirth, W.: Solar Phys. **48** (1976) 41.
76Kus Kuseski, R.A., Swanson, P.N.: Solar Phys. **48** (1976) 41.
77Dul Dulk, G.A., Sheridan, K.V., Smerd, S.F., Withbroe, G.L.: Solar Phys. **52** (1977) 349.
77Eri Erickson, W.C., Gergeley, T.E. Kundu, M.R., Mahoney, M.J.: Solar Phys. **54** (1977) 57.
77Kun1 Kundu, M.R., Gergeley, T.E., Erickson, W.C.: Solar Phys. **53** (1977) 489.
77Kun2 Kundu, M.R., Sou-Yang, L., McCulbough, T.P.: Solar Phys. **51** (1977) 321.
78Hac Hachenberg, O., Steffen, P., Harth, W.: Solar Phys. **60** (1978) 105.
78Tro Trottet, G., Lantos, P.: Astron. Astrophys. **70** (1978) 245.
81Hac1 Hachenberg, O.: Landolt-Börnstein, New Series VI/2a (1981) 106.
81Hac2 Hachenberg, O.: Landolt-Börnstein, New Series VI/2a (1981) 287.
85She Sheridan, K.V., McLean, D.J.: in: *Solar Radiophysics* (1985) (eds. D.J. McLean, N.R. Labrum), Cambridge University Press, p. 443.
86Kun Kundu, M.R., Melozzi, M., Shevgaonkar, R.K.: Astron. Astrophys. **167** (1986) 166.
87Lan Lantos, P., Alissandrakis, C.E., Gergely, T., Kundu, M.R.: Solar Phys. **112** (1987) 325.
88Gar Gary, D.E., Zirin, H.: Astrophys. J. **329** (1988) 991.
88Mel Melrose, D.B., Dulk, G.A.: Solar Phys. **116** (1988) 141.
91Zir Zirin, H., Baumert, B.M., Hurford, G.J.: Astrophys. J. **370** (1991) 779.
92Bor Borovik, V.N., Kurbanov, M.S., Makarov, V.V.: Soviet Astr. **36** (1992) 656.
97Ben Benz, A.O., Krucker, S., Acton, L.W., Bastian, T.S.: Astron. Astrophys. **320** (1997) 993.
99Bra Brajsa, R., Ruzdjak, V., Vrsnak, B., Wöhl, H., Pohjolainen, S., Urpo, S.: Solar Phys. **184** (1999) 281.
00Kru Krucker, S., Benz, A.O.: Solar Phys. **191** (2000) 341.
01Tap Tapping, K.F., Zwaan, C.: Solar Phys. **199** (2001) 317.
04Chi Chiuderi, A., Chiuderi Drago, F.: Astron. Astrophys. **422** (2004) 331.
07Tap Tapping, K.F., Boteler, D., Charbonneau, P., Crouch, A., Manson, A., Paquette, H.: Solar Phys. **246** (2007) 309.
08Fiv Fivian, M.D., Hudson, H.S., Lin, R.P., Zahid, H.J.: Science **322** (2008) 560.
08Pen Penticton 10.7 cm flux density: see http://www.ngdc.noaa.gov/stp/SOLAR/FLUX/flux.html.
08Tap Tapping, K.: NRC, Penticton, BC, Canada, (2008) personal communication.
08The Thejappa, G., MacDowall, R.J.: Astrophys. J. **676** (2008) 1338.
08Zha Zhao, J., Han, Y.-B.: Chin. J. Astron. Astrophys. **8** (2008) 472.